J Mol Model (2013) 19:697–704
DOI 10.1007/s00894-012-1595-9

ORIGINAL PAPER

Molecular dipole effects on tuning electron transfer in a porphine–quinone complex: a DFT and TDDFT study

Oana Cramariuc · Pekka J. Aittala · Terttu I. Hukka

Received: 27 June 2012 / Accepted: 30 August 2012 / Published online: 26 September 2012

Abstract The effect of a strong electric field generated by molecular dipoles on the ground state electronic structure and the Q and B states as well as the lowest charge transfer (CT) excited state of porphine–2,5-dimethyl-1,4-benzoquinone (PQ) complex has been investigated theoretically. Density functional theory DFT and time-dependent DFT (TDDFT) with the BH&HLYP hybrid functional have been applied in these calculations. The molecular dipole effect was generated by imposing one or two helical homopeptides consisting of eight α-aminoisobutyric acid residues (Aib_8) close to the PQ complex. The molecular dipoles in a close proximity to the PQ complex expose it to an electric field of the order of magnitude of 10^9 V/m. The presence of the ambient molecular dipoles affects mainly the energy of the lowest CT state and barely the energies of the Q and B states. The molecular dipoles affect the energies of the excited states in a similar way as an external electrostatic field. Hence, the electric field induced by the molecular dipoles of the helical peptides could be used analogously to the external electrostatic field to control electron transfer (ET) in the PQ complex.

O. Cramariuc
Department of Physics, Tampere University of Technology,
P.O. Box 692, 33101 Tampere, Finland

P. J. Aittala · T. I. Hukka (✉)
Department of Chemistry and Bioengineering, Tampere University of Technology,
P.O. Box 541, 33101 Tampere, Finland
e-mail: terttu.hukka@tut.fi

O. Cramariuc
IT Center for Science and Technology,
Av. Radu Beller 25,
Bucharest, Romania

Keywords BH&HLYP · Electron transfer · Peptide · Porphine–quinone complex · TDDFT

Introduction

Inspired by natural photosynthesis and driven by the increasing need for clean energy sources, the field of organic solar cells based on artificial photosynthetic reaction centers has seen an exponential growth in publications over the last years. The initial steps in converting solar energy can be described by elementary photophysical processes, the essential ones being absorption of light by a chromophore and electron transfer (ET) from the photoexcited electron donor to an acceptor. The initial ET is a starting point of several subsequent electron transfer reactions which lead to long-living charge-separated states [1]. In a previous study we have shown that ET in an artificial photosynthetic reaction center modeled by porphine and quinone can be tuned by an external electric field to which the system has been exposed [2]. It was proven by employing TDDFT/BH&HLYP and approximate coupled cluster singles and doubles (CC2) methods that field strengths of the order of 10^9 V/m can be used to induce or prevent conical intersections (CIs) between the locally excited porphine states and the energetically lowest charge transfer (CT) state. Dipole-assisted exciton dissociation is also supported by density functional theory (DFT) calculations [3] in which the electronic structure has been investigated at a polymer/fullerene interface. At the same time, experimental work on various photosynthetic reaction centers, including porphyrin-fullerene dyads [4], shows acceleration and deceleration of photoinduced electron transfer rates by electric fields [5, 6].

In the present article we extend our previous study [2] by using instead of an external electric field real molecules that

presumably have a similar electric effect on ET between the two moieties of the considered porphine–2,5-dimethyl-1,4-benzoquinone (PQ) complex. Thus, we aim to answer the question whether it is possible to design real molecular systems in which the effect of an electric field is generated by ambient molecules surrounding the artificial photosynthetic reaction center models. As speculated in our previous study [2] and suggested by some publications [7–10] dealing with this subject, molecular dipoles of helical peptides could be good candidates for creating the desired electric field to which the PQ complex is exposed. The Aib_8 polypeptide, consisting of eight α-aminoisobutyric acid residues, was selected for this study because the Aib residues are reported as strong helix formers in peptides. Two methyl groups, which are attached to α-carbon of Aib, restrict the conformational space of the residues and as a result the α- or 3_{10}-helix structure is usually favored [11, 12].

The geometry of the Aib_8 has been obtained from the crystal structure of Z-$(Aib)_{11}$-O*t*Bu [11] by optimizing the peptide chain at the level of density functional theory (DFT) using the PBE functional, which has been shown to yield good geometries for polyglycine [13]. The SV(P) basis set (comparable to 6-31G*) was used in the DFT calculations, because the 6-31G(d) basis set has been reported to provide structural parameters already comparable to the larger 6-311+G(d,p) basis set [13]. In addition, the calculated dipole moments and electric fields were verified by using the larger TZVP basis set.

While high level multi-configurational self-consistent field methods are needed for an accurate description of ET in the vicinity of CIs, even CC2 calculations proved to be too demanding for the combined PQ and peptide system. Especially since a relatively large basis set and active space are needed in the CC2 calculations for achieving the correct picture of the excited states [2]. Therefore, the present calculations of the excited states have been carried out using TDDFT with the BH&HLYP functional, which has been shown to yield reasonable results for long range ET processes, due to the larger portion of HF exchange [14]. The SV(P) basis set has also been used in the TDDFT calculations. The validity of this basis set in the excited state energy calculations of the PQ complex has been confirmed by calculations with the TZVP basis set [2].

Computational methods

The ground state geometry optimizations and the single-point dipole moment and molecular orbital (MO) calculations were carried out with density functional theory (DFT) [15, 16]. The ground state geometry of the Aib_8 homopeptide was obtained by a following procedure. A chain with eight Aib residues was extracted from the crystal structure of the Z-$(Aib)_{11}$-O*t*Bu [11]. The N- and C-termini were capped with a hydrogen atom and a hydroxyl group, respectively. Finally, the geometry of the Aib_8 was optimized by using the GGA type PBE [17–20] functional. The DFT/B3LYP/SV(P)-optimized ground state geometry of the $PQ_{5.0}$ complex reported in our previous study [2] was used in the calculations. The electronic structures were studied by performing single-point calculations with the "half-and-half" hybrid functional BH&HLYP [17, 18, 21–23] (BHandHLYP). The Karlsruhe split valence basis set with one set of polarization functions for all atoms except for hydrogen (SV(P)) [24] (roughly 6-31G*) was applied in all DFT calculations employing PBE and BH&HLYP, while larger triple-ζ basis with polarization functions on all atoms (TZVP) [25] (comparable to 6-311G**) was used to verify the calculated dipole moments of the Aib_8 chain.

Vertical excitation energies were calculated with the time-dependent DFT (TDDFT) [26–28] by using the BH&HLYP functional with the SV(P) basis set. Only the singlet states were considered. All calculations were performed with the TURBOMOLE versions 6.0 and 6.1 [29].

Results and discussion

Geometries of the Aib_8 homopeptides

Some structural characteristics of the Aib_8 homopeptide optimized at the DFT/PBE/SV(P) level are presented in Table 1 together with those of the crystalline Z-$(Aib)_{11}$-O*t*Bu [11] and the infinitely long Aib 3_{10}- and α-helices (AibIH) calculated with DFT using periodic boundaries (PBC) [12]. The definitions of the angle τ and torsion angles ψ, φ, and ω are illustrated in Fig. 1.

The quite perfect 3_{10}-helix form of Z-$(Aib)_{11}$-O*t*Bu is distorted when the structure is optimized with DFT in vacuum. This is expected, because of the known shortcomings of current DFT functional, for example such as the missing van der Waals interactions, and because the structure of the peptide is more tightly packed in a crystal than in vacuum. In contrast to the crystalline structure, the DFT-optimized Aib_8 structure is slightly unfolded and the structure is actually an intermediate between the 3_{10}- and α-helices. The residues per turn ratio 3.43 and the twist per residue ratio 104.96° of Aib_8 are closer to those of a perfect α-helix (3.6 and 100°) than those of a 3_{10}-helix (3 and 120°). However, the dihedral angles ψ (–26.4°) and φ (–52.4°) as well as the angle τ (111.4°) of Aib_8 agree with the corresponding parameters of the 3_{10}-helical form of AibIH (–25.3°, –51.3°, and 111.4°) better than with those of α-helical form (–43.8°, –55.4°, and 109.9°). Only the dihedral angle ω (175.8°) of Aib_8 agrees better with that of the α-helical form of AibIH (175.6°) than that of the 3_{10}-helix (177.5°). The

Table 1 Some (average) optimized structural characteristics of the Aib_8 peptide. In addition, the characteristics of the infinitely long 3_{10}- and α-helices (AibIH) and of the crystalline Z-$(Aib)_{11}$-O*t*Bu are shown for comparison. Length is given in Angstroms and angles are given in degrees

Helix type	Aib_8[a]	AibIH[b]		Z-$(Aib)_{11}$-O*t*Bu[c]
		3_{10}	α	3_{10}
length	18.724			
number of turns	2.33			
< residues / turn >	3.43			3.06
< rise / residue >	2.34	2.00	1.72	1.98
< helical twist / residue >	104.96			117.73
$<\psi>$	−26.4	−25.3	−43.8	−27±4
$<\varphi>$	−52.4	−51.3	−55.4	−53±4
$<\omega>$	175.8	177.5	175.6	179±3
$<\tau>$	111.4	111.4	109.9	

[a] Calculated at the DFT/PBE/SV(P) level of theory

[b] Calculated at the PBC/DFT/PBE/6-31G(d) level of theory, see ref. [12]

[c] Experimental values from ref. [11]

4→1 hydrogen bonding observed in Aib_8 is characteristic for 3_{10}-helices. The unfolding lengthens the peptide chain as can be seen from the rise per residue values of 2.34 Å and 1.98 Å for Aib_8 and Z-$(Aib)_{11}$-O*t*Bu, respectively. Apart from the unfolding, the structure of the Aib_8 remains well defined as can be seen from Fig. 2.

Because it is the internal electric field of the Aib_8 that is expected to perturb the electronic structure and the excited states of the PQ complex and the electric field is induced by the dipole moment of the peptide, the calculated dipole moment is actually more interesting than the optimized geometries of the peptide. In agreement with the previous investigations [9, 30], the computed dipole is oriented along the helix axis and points from the C-terminus to the N-terminus, as sketched in Fig. 2. The dipole moment computed at the PBE/SV(P) level is 31.0 D (1 D ≈ 3.33564×10^{-30} Cm), which is slightly more than the 3.5 D value per amino acid residue reported for α-helices [5]. Because the electronic

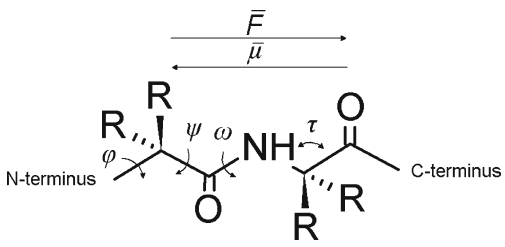

Fig. 1 Schematic structure of a homopeptide chain illustrating the angle τ and torsion angles ψ, φ, and ω. In addition, the directions of the dipole moment μ and the induced electric field F are shown. In Aib polypeptides the substituents R are methyl groups -CH_3

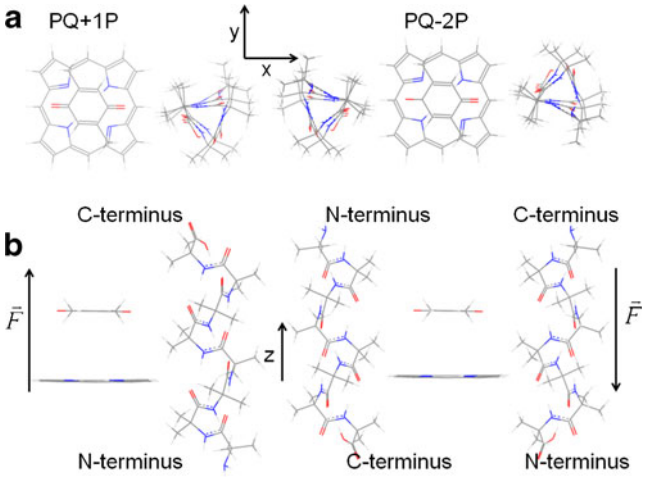

Fig. 2 Top-view **a** and side-view **b** of PQ+1P (left) and PQ-2P (right). The direction of the electric field induced by the ambient peptides is indicated by an arrow. Carbon atoms are gray, oxygens red, nitrogens blue, and hydrogens light gray

structure calculations of the PQ complex are carried out by using the BH&HLYP functional with the SV(P) basis set, it is also important to check the dipole moment at the same level. The DFT/BH&HLYP/SV(P) calculations yield an estimate of 33.6 D for the dipole moment. However, the SV(P) basis set is rather small and the basis set size may have a significant influence on the calculated dipole moment [31]. Thus, single-point calculations were carried out for the Aib_8 homopeptide also at the BH&HLYP/TZVP//PBE/SV(P) level in order to verify the calculated dipole moment. The dipole moment obtained at the BH&HLYP/TZVP//PBE/SV(P) level, 34.0 D, is only slightly larger than that obtained by using the SV(P) basis set. Moreover, the orientation of the dipole moment is not affected by the basis set. Thus, in this particular case the basis set and functional have only little influence on the calculated dipole moment.

Strength of the electric field induced by the Aib_8 homopeptides

The porphine–quinone–Aib_8 system was constructed from the optimized geometries of the PQ complex and an Aib_8 homopeptide. Either one or two Aib_8 chains were placed next to the PQ complex such that the helix axis is parallel to the axis pointing from the geometric center of the porphine to the geometric center of quinone. In addition, the C-terminus was set either to the porphine or quinone side of the complex. Consequently four different systems, denoted as PQ–1P, PQ–2P, PQ+1P, and PQ+2P were constructed. In PQ–1P the N-terminus of Aib_8 is on the quinone side of the PQ complex such that the electric field induced by the peptide points from quinone to porphine, see Fig. 2. Thus, it is expected that this alignment would favor CT from porphine to quinone (the direction of the electric field is defined as a direction of the

movement of a positive charge). In PQ–2P, there are two peptide chains with the PQ complex in the middle of them and the orientations of the Aib_8 chains with respect to the PQ complex are identical to that in PQ–1P. In PQ+1P and PQ+2P one or two Aib_8 chains, respectively, are oriented such that the N-terminus is on the porphine side of the PQ complex, see Fig. 2. In these systems the electric field induced by the molecular dipoles of the peptide chains is expected to prevent the CT from porphine to quinone.

In order to estimate the field induced by the peptides only, the strength of an electric field induced by the Aib_8 homopeptides in PQ–1P, PQ–2P, PQ+1P, and PQ+2P systems was calculated without the PQ complex. The electric fields, calculated at the DFT/BH&HLYP/SV(P) level of theory at the location which would be in between the geometric centers of porphine and quinone, were –1.100, –0.580, +0.580, $+1.100\times10^9$ V/m in the PQ–1P, PQ–2P, PQ+1P, and PQ+2P systems, respectively. Minus corresponds to the direction from quinone to porphine and plus the direction from porphine to quinone, just as in the case of the external electrostatic field [2]. The calculated electric fields induced by the Aib_8 homopeptides are of the same order of magnitude (10^9 V/m) as the maximum proposed for the helical peptides on the basis of vacuum electrostatics [9].

As expected on the basis of the dipole moment of Aib_8, in each system the direction of the induced field is parallel to the helix axis of the peptides. In PQ–1P and PQ+1P the *x* (-0.131×10^9 V/m) and *y* (+0.051 and -0.051×10^9 V/m, respectively) components have only a small contribution to the norm of the field. Moreover, in PQ–2P and PQ+2P the *x* and *y* components of the electric field practically cancel out because of the symmetry. Hence it is the *z* components (–1.100, –0.560, +0.560, $+1.100\times10^9$ V/m in PQ–1P, PQ–2P, PQ+1P, and PQ+2P, respectively) that determine the direction of the electric field induced by the Aib_8 homopeptides. Because the electric field induced by the Aib_8 helices is parallel to the helix axis, in PQ–1P, PQ–2P, PQ+1P, and PQ+2P the influence of the induced field is the highest possible and any change in the alignment of the Aib_8 chains with respect to the PQ complex would decrease the effect of the ambient peptides.

The accuracy of the electric fields calculated with the SV(P) basis set was verified by further calculations with the TZVP basis set. The strengths of the electric fields in the PQ–1P, PQ–2P, PQ+1P, and PQ+2P systems calculated at the BH&HLYP/TZVP level, –1.104, –0.586, +0.586, and $+1.104\times10^9$ V/m, respectively, are in excellent agreement with those obtained by using the SV(P) basis set. In addition, the *z* components (1.104, –0.567, +0.567, $+1.104\times10^9$ V/m) calculated with the TZVP basis set agree with those calculated with SV (P). Thus, the SV(P) basis set was used throughout the remaining calculations.

The influence of the molecular dipoles of the ambient Aib_8 peptides on the electronic structure of the PQ complex

The influences of the electric fields induced by the ambient peptide chains on the molecular orbital (MO) energies of the PQ complex were studied by performing single-point calculations at the DFT/BH&HLYP/SV(P) level of theory for the PQ–1P, PQ–2P, PQ+1P, and PQ+2P systems. The PQ complex with the intermolecular distance set to 5.0 Å ($PQ_{5.0}$), here referred to just as PQ, was chosen for a closer inspection because the influence of an external electric field increases when the intermolecular distance increases [2]. The influence of the molecular dipole of the ambient peptides on the energies of the two highest occupied and three lowest unoccupied MOs of the PQ complex calculated with BH&HLYP is presented in Fig. 3a. In addition, the influences of the external electrostatic fields of ±0.5 and $\pm1.0\times10^9$ V/m are shown for comparison in Fig. 3b. The isoamplitude surfaces of HOMO–1, HOMO, LUMO, LUMO+1, and

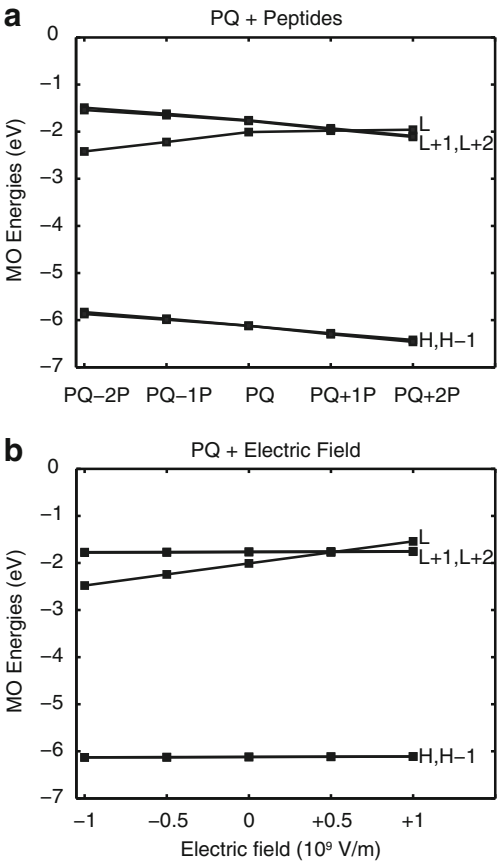

Fig. 3 The influence of **a** the ambient peptide chains and **b** the static external electric field (adopted from ref. [2]) on the orbital energies in the PQ complex calculated at the DFT/BH&HLYP/SV(P) level of theory. See Fig. 2 for the structures of the systems and for the directions of the induced electric fields in PQ–2P, PQ–1P, PQ+1P, and PQ+2P. The static external electric field is aligned perpendicular to the porphine and quinone planes, *i.e.* along the *z*-axis defined in Fig. 2

LUMO+2 of the PQ–1P system are presented in Fig. 4. In other systems the localization of the MOs is similar to that of PQ–1P shown in Fig. 4 and thus the MOs of the other systems are not shown.

An external electrostatic field was shown to affect the energies of the orbitals localized mostly on quinone, whereas the orbitals localized entirely on porphine were affected hardly at all [2]. However, depending on the system, the Aib_8 peptide influences the MOs localized either on porphine or on quinone. In the systems where the induced field is directed from quinone to porphine, that is, PQ–1P, PQ–2P, the field affects the energies of the MOs localized on quinone (LUMO) more than the energies of the MOs localized on porphine (HOMO–1, HOMO, LUMO+1, and LUMO+2). On the contrary, in the systems where the induced field is directed from porphine to quinone, that is, PQ+1P, PQ+2P, the field affects the energies of the MOs localized on porphine whereas the energies of the MOs localized on quinone are affected less. This different behavior as compared to the external electrostatic field suggests interaction of the peptide molecules with the PQ complex and eventual coupling of their MOs.

The HOMO, HOMO–1, LUMO+1, and LUMO+2 energies of PQ–1P are only 0.06 eV larger than those of PQ. Furthermore, in PQ–2P the energies of these MOs are 0.07–0.10 eV higher than in PQ–1P. In contrast, the energy of LUMO in PQ–1P and PQ–2P is 0.23 and 0.44 eV lower, respectively, than in PQ. Consequently, the HOMO–LUMO gap is 0.34 and 0.70 eV smaller in PQ–1P and PQ–2P than in PQ (4.11 eV). The molecular dipoles of the peptides influence the HOMO–LUMO gap of PQ–1P and PQ–2P more strongly than expected on the basis of the strength of the induced electric field (–0.580 and -1.100×10^9 V/m, respectively) because the static electric fields of –0.5 and -1×10^9 V/m decrease the HOMO–LUMO gap only by 0.23 and 0.46 eV, respectively (see Fig. 3).

In PQ+1P the energies of HOMO, HOMO–1, LUMO+1, and LUMO+2 are 0.17 eV smaller than those in PQ. Furthermore, the energies of these MOs of PQ+2P decrease by 0.22 eV from those of PQ+1P. However, the energy of LUMO is 0.05 eV higher in PQ+1P than in PQ. Moreover, the energy of LUMO is the same in the PQ+1P and PQ+2P systems. As a result, the HOMO–LUMO gap is 0.18 and 0.35 eV larger in PQ+1P and PQ+2P than in PQ (4.11 eV), respectively, which is less than expected on the basis of the strength of the induced electric field (+0.580 and $+1.100\times10^9$ V/m, respectively) because the static electric fields of +0.5 and $+1\times10^9$ V/m increase the HOMO–LUMO gap by 0.23 and 0.46 eV, respectively. However, in both cases, *i.e.* with the external electrostatic field and the field induced by the peptides, the HOMO level crosses the LUMO+1 and LUMO+2 levels roughly at the same field strength, that is, at slightly over $+0.5\times10^9$ V/m.

As a conclusion, the external electrostatic field affects only the energies of the MOs localized on quinone whereas the ambient peptides affect the MOs localized both on porphine and quinone. However, both the external electrostatic field and the peptides affect the relative energies of the MOs of the PQ complex localized on porphine and quinone in a surprisingly similar way. Therefore, on the basis of the preceding MO analysis, it seems possible to use high electric fields induced by peptides to control the CT states of the PQ systems analogously to controlling by external electrostatic fields.

The influence of the molecular dipoles of the ambient Aib_8 peptides on the excited states of the PQ complex

The energies of the Q_x, Q_y, B_x, and B_y states as well as that of the lowest CT state of the PQ complex in the PQ–1P, PQ–2P, PQ+1P, and PQ+2P systems calculated by using TDDFT with the BH&HLYP functional are presented in Table 2. The corresponding excitation energies of the PQ complex calculated in a zero field and in the presence of external electric fields of ±0.5 and $\pm1.0\times10^9$ V/m are shown for comparison. The Q_x, Q_y, B_x, and B_y states of PQ–1P, PQ–2P, PQ+1P, and PQ+2P were confirmed as the locally excited porphine states by calculating the electron density difference between the ground state and the excited state. In addition, the electron density difference between the ground state and the proposed lowest CT state show how the charge is shifted from porphine to quinone, see Fig. 5.

Molecular dipoles of ambient Aib_8 homopeptides and external electrostatic fields have somewhat similar effects on the energies of the excited states of the PQ complex. The electric field induced by the ambient Aib_8 peptide chains affects the energies of the localized porphine (Q_x, Q_y, B_x, and B_y) states slightly, contrary to the external electrostatic field, which has hardly any effect on these states. However, the changes in the

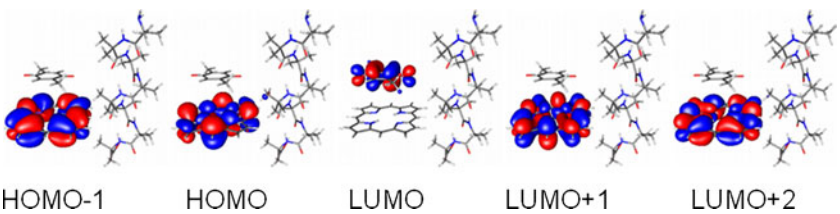

Fig. 4 Some of the orbitals of the PQ–1P system calculated at the BH&HLYP/SV(P) level of theory. The isoamplitude surfaces of the orbitals presented are 10 % of the maximum positive (red) and minimum negative (blue) amplitudes of the wave functions

Table 2 Excitation energies (eV) of the Q_x, Q_y, B_x, and B_y states as well as of the lowest CT state of the PQ complex in zero field, in the presence of an external electric field[a], and in the presence of the ambient Aib_8 homopeptides[b]

State	PQ[c]	PQ+electric field				PQ+peptides			
	Zero field	−1[c]	−0.5	+0.5	+1[c]	PQ–2P	PQ–1P	PQ+1P	PQ+2P
Q_x	2.26	2.26	2.26	2.26	2.26	2.25	2.26	2.26	2.25
Q_y	2.45	2.45	2.45	2.45	2.45	2.43	2.44	2.44	2.43
CT	2.92	2.46	2.69	3.15	3.38	2.22	2.56	3.10	3.27
B_x	3.61	3.61	3.61	3.61	3.61	3.56	3.59	3.59	3.56
B_y	3.73	3.73	3.73	3.73	3.73	3.67	3.70	3.70	3.67

[a] ±0.5 and $\pm 1 \times 10^9$ V/m

[b] Calculated at the TDDFT/BH&HLYP/SV(P) level of theory

[c] From ref. [2]

energies of the Q and B states are small compared to the changes in the energy of the lowest CT state, see below. Moreover, the relative order of the states is the same both under the influences of the fields induced by the ambient peptides and of the external electrostatic fields of similar strengths.

The energies of the Q and B states of the PQ–2P, PQ–1P, PQ+1P, and PQ+2P systems are 0.06 eV smaller than those of the isolated PQ complex at most. When the peptides are present the energy difference between the orbitals involved in the one electron excitations, *i.e.* from HOMO to LUMO+1 and HOMO–1 to LUMO+2, which form the Q and B states, respectively, decreases. Contrary to this, as mentioned above the external electrostatic field hardly influences the energies of these orbitals and therefore of the states, see Fig. 3a and "The influence of the molecular dipoles of the ambient Aib_8 peptides on the electronic structure of the PQ complex." In the presence of peptides, the energy difference between the almost degenerate HOMO and HOMO–1 and the almost degenerate LUMO+1 and LUMO+2 is 0.02 eV smaller in PQ–1P and 0.01 eV smaller in PQ+1P than in PQ. This energy difference decreases further by the same amount in the cases of PQ–2P and PQ+2P, *i.e.* by 0.04 and 0.02 eV, respectively, in relation to PQ.

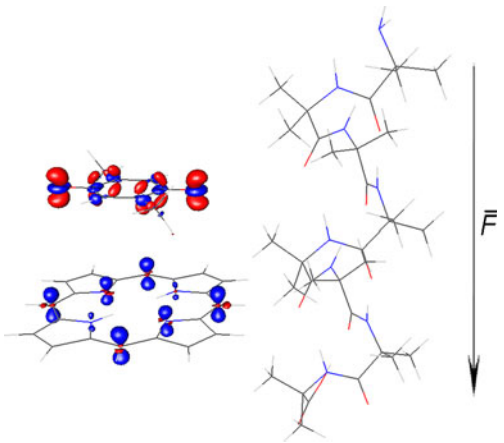

Fig. 5 Electron density difference between the ground state and the lowest CT state in the PQ–1P system. Blue represents areas with more negative charge in the ground state as compared to the CT state, while red represents areas with more negative charge in the CT state

Molecular dipoles of ambient peptides affect the energy of the lowest CT state in a similar way as the external electrostatic field. The presence of the peptides decreases the energy of the CT state in PQ–1P and PQ–2P compared to the unperturbed PQ complex as in the case of a negative external electrostatic field. However, the quantitative decrease of the energy of the CT state is bigger than in the cases of the –0.5 and -1.0×10^9 V/m static fields, see Table 2. Thus, the ambient Aib_8 chains influence the PQ–1P and PQ–2P systems more strongly than expected on the basis of the strengths of the electric fields induced by the peptides (–0.580 and -1.100×10^9 V/m in PQ–1P and PQ–2P, respectively). However, the energy of the lowest CT state decreases by precisely the same amount as the HOMO–LUMO gap in PQ–1P and PQ–2P in relation to the gap of the unperturbed PQ complex, namely by 0.36 and 0.70 eV, respectively.

The energy of the CT state is higher in PQ+1P and PQ+2P than in the unperturbed PQ complex just as in the case of the positive external electrostatic field. However, the external electrostatic fields of +0.5 and $+1.0 \times 10^9$ V/m increase the energy of the CT state of the PQ complex more strongly than the ambient Aib_8 chains in PQ+1P and PQ+2P. As in the case of the PQ–1P and PQ–2P systems, the molecular dipoles of the peptides increase the energy of the lowest CT state in PQ+1P and PQ+2P by the same amount as that of the HOMO–LUMO gap, that is, by 0.18 and 0.35 eV, respectively, in relation to the unperturbed PQ complex.

The influence of the molecular dipoles of the ambient Aib_8 peptides on the electron transfer in the PQ complex

We have previously shown that it is possible to control the crossings of the locally excited porphine states (Q and B)

and the lowest porphine-to-quinone CT state by applying an external electric field of the order of magnitude of 10^9 V/m [2], see Fig. 6. These crossings can correspond to the CI between the states which would facilitate an efficient ET from porphine to quinone when either the Q or B state of the porphine moiety is photoexcited. As discussed in "The influence of the molecular dipoles of the ambient Aib_8 peptides on the excited states of the PQ complex," the electric field induced by the Aib_8 homopeptides is of the same order of magnitude and has a similar effect on the excited states of the PQ complex as the external electrostatic field. Thus, analogously to the case of the external electrostatic field, it would be possible to control the crossings of the PECs of the locally excited porphine states (Q and B) and the lowest CT state by using the perturbation created by the ambient Aib_8 chains. In the current investigation we have found that one Aib_8 chain orienting the N-terminus to the quinone side of the PQ complex has roughly the same effect as the external electrostatic field of -0.8×10^9 V/m. At the same time, because the presence of one or two Aib_8 chains orienting the C-terminus to the quinone side decreases the energies of the B states and increases the energy of the CT state slightly, one Aib_8 chain orienting the C-terminus to the quinone side has roughly the same overall effect on the gaps between the CT and B states as an external electrostatic field of $+0.4\times10^9$ V/m.

The PECs of the Q states and the lowest CT state calculated with BH&HLYP cross under the influence of an external electrostatic field strength of *ca.* -1×10^9 V/m (Fig. 6). Thus, already two ambient Aib_8 chains (PQ–2P) are enough to shift the PEC of the lowest CT state close to the PECs of the Q states and cause crossing of these states, see also Table 2. The PECs of the B states and the lowest CT state cross under the influence of an external electrostatic field strength of $+2.0\times10^9$ V/m. Because, according to the calculations employing BH&HLYP, one Aib_8 chain in PQ+1P and PQ+2P has a milder effect than the external electrostatic field of $+1\times10^9$ V/m on the energy of the lowest CT state, it would require four or even more Aib_8 homopeptides in close proximity to the PQ complex to induce the crossings of the B states with the lowest CT state.

Comparison to the PECs obtained with the CC2 method has shown [2], however, that BH&HLYP underestimates the CT energy. On the basis of the PECs calculated at the CC2/TZVP level of theory under the influences of external electrostatic fields of various strengths it seems that already the presence of one Aib_8 homopeptide would be enough to induce the crossings of the B states with the lowest CT state because the PEC of the CT state lies very close to the PECs of the B states already in zero field (see Fig. 6). Furthermore, because one Aib_8 chain orienting the N-terminus to the quinone side of the PQ complex has roughly the same effect as the external electrostatic field of -0.8×10^9 V/m,

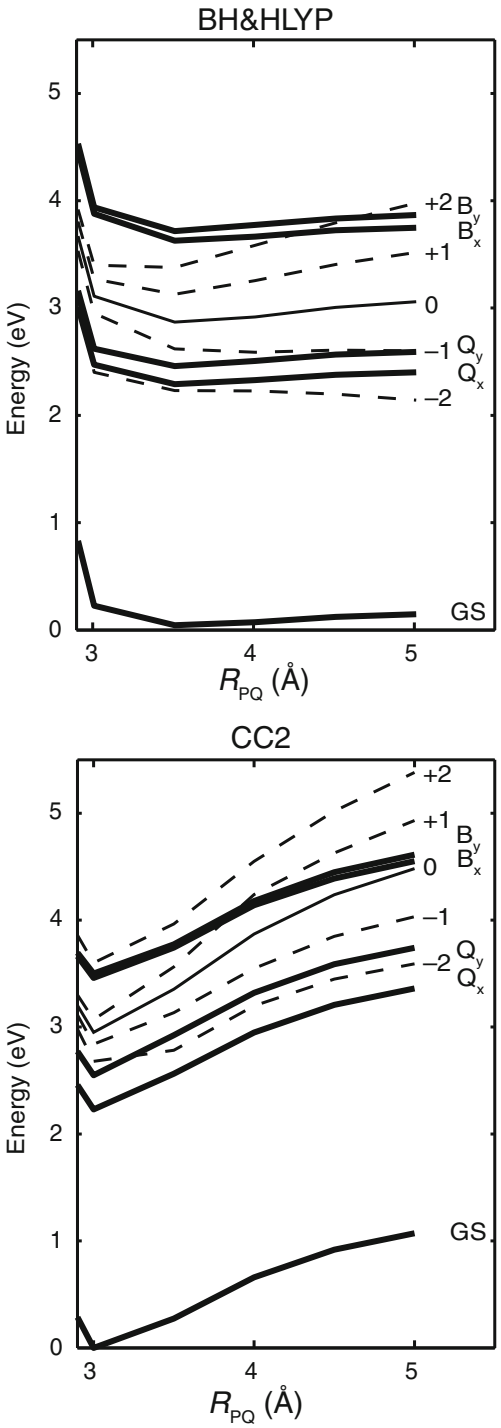

Fig. 6 PECs of the ground state (GS), the Q_x, Q_y, B_x, and B_y states, and the energetically lowest CT state of the PQ complex as a function of the intermolecular distance R_{PQ} calculated in zero field. Additionally, the PECs of the lowest CT state calculated under the influences of external electric fields of ±1 and $\pm2\times10^9$ V/m are shown. The curves are adopted from ref. [2] and have been calculated at the TDDFT/BH&HLYP/SV(P) and CC2/TZVP levels of theory

which is in agreement with the TDDFT/BH&HLYP calculations, the CC2 calculations predict that the perturbation

created by two peptides would induce the crossings of the CT and Q states.

As a conclusion, according to the calculations performed in this study it would be possible to select a locally excited state (either Q or B) whose photoexcitation leads to ET from porphine to the quinone moiety of the PQ complex. This could be achieved by introducing one or two ambient Aib_8 homopeptides in close proximity to the PQ complex and by changing the orientations of the ambient homopeptides with respect to porphine and quinone, that is, PQ–1P (Q states) versus PQ+2P (B states).

Conclusions

In this article we have investigated the influence of the electric field induced by molecular dipoles of one or two short ambient helical Aib_8 homopeptide chains on the ground state electronic structure and the excited states of the porphine–quinone complex by using DFT and TDDFT with the BH&HLYP functional. Two different relative orientations of the ambient Aib_8 chains with respect to the PQ complex have been studied: the first one in which the C-terminus is on the quinone side of the PQ complex and the field induced by the peptides is directed from porphine to quinone and the second one in which the orientations are opposite.

The electric field induced by the molecular dipoles of the ambient peptides from their N-terminus to the C-terminus is of the order of magnitude of 10^9 V/m and is practically parallel to the helix axis. The overall effect of the peptide-induced electric field on the energies of the MOs of the PQ complex is very similar to that of the external electrostatic field. However, depending on the relative orientation with respect to the PQ complex the molecular dipoles of the ambient peptides affect either the MOs localized on porphine or quinone, whereas the external electrostatic field affects the energies of the MOs localized on quinone only. Additionally, the molecular dipoles of the peptides influence the HOMO–LUMO gap energy more strongly in PQ–1P and PQ–2P and more weakly in PQ +1P and PQ+2P than expected on the basis of the strengths of the electric fields induced by the molecular dipoles of the ambient helical peptides.

The ambient Aib_8 peptides generate perturbations which affect the energies of the locally excited porphine Q and B states clearly less than that of the lowest CT state of the PQ complex. One Aib_8 chain orienting the N-terminus to the quinone side of the PQ complex has roughly the same effect on the energy of the CT state as the external electrostatic field of -0.8×10^9 V/m, whereas one Aib_8 chain orienting the C-terminus to the quinone side has roughly the same effect as the external electrostatic field of $+0.4\times10^9$ V/m. Because the induced electric field has a similar effect on the excited states of the PQ complex as the external electrostatic field, it would be possible to control the crossings of the PECs of the locally excited porphine states (Q and B) and the lowest CT state by using the perturbation created by the ambient Aib_8 peptide chains. Hence, the ambient Aib_8 homopeptides can be used analogously to the external electric field to control the ET in the PQ complex.

Acknowledgments Prof. H. Lemmetyinen, the head of the Laboratory of Chemistry at Tampere University of Technology, is acknowledged for offering the facilities for this research. Computing resources provided by the CSC – IT Center for Science Ltd, administrated by the Finnish Ministry of Education, are acknowledged. Financing of this research by the Academy of Finland is greatly appreciated.

References

1. Hoff AJ, Deisenhofer J (1997) Phys Rep 287:1–247
2. Aittala PJ, Cramariuc O, Hukka TI (2010) J Chem Theory Comput 6:805–816
3. Marchiori CFN, Koehler M (2010) Synt Met 160:643–650
4. Ohta N, Mikami S, Iwaki Y, Tsushima M, Imahori H, Tamaki K, Sakata Y, Fukuzumi S (2003) Chem Phys Lett 368:230–235
5. Kimura S (2008) Org Biomol Chem 6:1143–1148
6. Nakabayashi T, Hino K, Ohta Y, Ito S, Nakano H, Ohta N (2011) J Phys Chem B 115:8622–8626
7. Hol WGJ (1985) Prog Biophys Mol Biol 45:149–195
8. Galoppini E, Fox MA (1996) J Am Chem Soc 118:2299–2300
9. Fox MA, Galoppini E (1997) J Am Chem Soc 23:5277–5285
10. Nakayama H, Morita T, Kimura S (2009) Phys Chem Chem Phys 11:3967–3976
11. Gessmann R, Brückner H, Petratos K (2003) J Peptide Sci 9:753–762
12. Improta R, Barone V, Kudin KN, Scuseria GE (2011) J Am Chem Soc 123:3311–3322
13. Improta R, Barone V, Kudin NK, Scuseria GE (2011) J Phys Chem 114:2541–2549
14. Magyar RJ, Tretiak S (2007) J Chem Theory Comput 3:976–987
15. Treutler O, Ahlrichs R (1995) J Chem Phys 102:346–354
16. von Arnim M, Ahlrichs R (1998) J Comput Chem 19:1746–1757
17. Dirac PAM (1929) Proc Royal Soc (London) A 123:714–733
18. Slater JC (1951) Phys Rev 81:385–390
19. Perdew JP, Wang Y (1992) Phys Rev B 45:13244–13279
20. Perdew JP, Burke K, Ernzerhof M (1996) Phys Rev Lett 77:3865–3868
21. Becke AD (1988) Phys Rev A 38:3098–3100
22. Lee C, Yang W, Parr RG (1988) Phys Rev B 37:785–789
23. Becke AD (1993) J Chem Phys 98:1372–1377
24. Schäfer A, Horn H, Ahlrichs R (1992) J Chem Phys 97:2571–2577
25. Schäfer A, Huber C, Ahlrichs R (1994) J Chem Phys 100:5829–5833
26. Bauernschmitt R, Ahlrichs R (1996) Chem Phys Lett 256:454–464
27. Bauernschmitt R, Häser M, Treutler O, Ahlrichs R (1997) Chem Phys Lett 364:573–578
28. Furche F, Ahlrichs R (2002) J Chem Phys 117: 7433–7447; (2004) J Chem Phys 121: 12772–12773 (E)
29. Ahlrichs R, Bär M, Häser M, Horn H, Kölmel C (1989) Chem Phys Lett 162:165–169
30. Sengupta D, Behera RN, Smith JC, Ullmann GM (2005) Structure 23:849–855
31. Koch W, Holthausen MC (2001) A chemist's guide to density functional theory, 2nd edn. Wiley-VCH, Weinheim